CHALMERS | UNIVERSITY OF GOTHENBURG

PREPRINT 2012:14

Adaptive approximate globally convergent algorithm with backscattered data

M. ASADZADEH
L. BEILINA

Department of Mathematical Sciences
Division of Mathematics
CHALMERS UNIVERSITY OF TECHNOLOGY
UNIVERSITY OF GOTHENBURG
Gothenburg Sweden 2012

Preprint 2012:14

Adaptive approximate globally convergent algorithm with backscattered data

M. Asadzadeh and L. Beilina

Department of Mathematical Sciences
Division of Mathematics
Chalmers University of Technology and University of Gothenburg
SE-412 96 Gothenburg, Sweden
Gothenburg, September 2012

Preprint 2012:14
ISSN 1652-9715

Matematiska vetenskaper
Göteborg 2012

Adaptive approximate globally convergent algorithm with backscattered data

M. Asadzadeh and L. Beilina

Abstract We construct, analyze and implement an approximatelly globally convergent finite element scheme for a hyperbolic coefficient inverse problem in the case of backscattering data. This extends the computational aspects introduced in [2], where using Laplace transformation, the continuous problem is reduced to a nonlinear elliptic equation with a gradient dependent nonlinearity. We investigate the behavior of the nonlinear term and discuss the stability issues as well as optimal a posteriori error bounds, based on an adaptive procedure, and due to the maximal available regularity of the exact solution. Numerical implementations justify the efficiency of adaptive a posteriori approach in the globally convergent setting.

1 Introduction

The inverse algorithms have a wide spectrum of application areas raging from mining, detecting oil reservoirs, earth layers, explosives in airports to medical optical imaging, etc. Efficiency of this problem, through *Approximate Globally Convergent Approximation (AGCA)* [22], was recently verified on blind imaging of the experimental data that was measured in picoseconds scale regime. In [2] we performed adaptive finite element technique directly inside the AGCA and derived optimal a posteriori error estimates for a finite element approximation of a nonlinear elliptic integro-differential equation. To further improving this efficiency we invoke an adaptivity procedure inside the AGCA algorithm, introduced in [2] for the numerical study of the hyperbolic coefficient inverse problem in two dimensions in the case of the full data collection.

Mohammad Asadzadeh; e-mail: mohammad@chalmers.se
Larisa Beilina; e-mail: larisa.beilina@chalmers.se
Department of Mathematics, Chalmers University of Technology and the University of Gothenburg, SE–412 96, Göteborg, Sweden

A direct numerical approach to solve coefficient inverse problems (CIP) is through a minimization procedure for the least square residual functional. This however, may lead to multiple local minima for the functionals. To avoid such an obstacle, in [20] a convexification algorithm was introduced for solution of the one-dimensional CIP in imaging electromagnetic frequency. This algorithm was further extended in [23] to higher dimensions with applications in diffusive optical mammography. Convexification is the origin of the AGCA methods. Some modified approaches to the AGCA algorithms were introduced in [6, 7, 8, 9] and summarized in [5], where a layer-stripping procedure was performed with respect to the pseudo-frequency rather than the spatial variable which is the case in the convexification. The Carleman weight function in [5, 6, 7, 8, 9] depends on the pseudo-frequency and not on the spatial variable, as in [20, 23]. These new approaches contribute to improved stability in the globally convergent reconstruction algorithm.

An alternative approach to solve CIP is a synthesis of a AGCA method and a strongly converging, however, local scheme such as the adaptive finite element method. In [7, 8] it was shown that the AGCA method provides a good initial guess for the locally convergent adaptive method. A first application of these results for the acoustic wave equation shows a good performance [7, 8, 9]. To compare with [7, 8, 9], the present work introduces extensive implementation results for a new such combination. Here adaptivity is performed directly inside the AGCA algorithm in the case when we have only backscattered data at the observation boundary.

A concise description of the theoretical procedure is as follows: A Laplace transformation in time converts the model problem to a convection-diffusion- type equation. The finite elements perform more accurately for elliptic and parabolic equations than the hyperbolic ones. Hence, the study of the CIP through combining a time transformation followed by a finite element procedure, not only reduces the dimension of the underlying problem, it also shifts the equation to a more desirable one from the finite element point of view. To our knowledge, the combination of the AGCA method, for a nonlinear elliptic problem and a posteriori procedure, using adaptive algorithm, is not considered elsewhere.

The paper is organized as follows: In Section 2 we formulate both forward and inverse problems and transfer the inverse problem to a Dirichlet boundary value problem for a nonlinear integro-differential equation with a removed unknown coefficient. In Section 3 we introduce the layer stripping procedure with respect to $s > 0$, the parameter of the Laplace transform in the original hyperbolic PDE. We point out that here we do not use the inverse Laplace transform, since approximations for the unknown coefficient are obtained in the "Laplace's domain". In Section 4 we describe a finite element method, state bounds for coefficients (derived in [2]) and formulate a corresponding dual problem. Section 5 is devoted to derivation of bounds for the nonlinear operator and a priori error estimates. In Section 6 we develop reliable and efficient a posteriori error estimates, for the full problem. In Section 7 we introduce a new adaptive globally convergent algorithm based on a posteriori error estimate of Section 6. Finally, in our concluding Section 8 we present the results of reconstruction of the function in two dimensions based on adaptive AGCA algorithm.

2 The forward and inverse problems

Consider the Cauchy problem for the hyperbolic equation

$$c(x)u_{tt} = \Delta u, \quad \text{in } \mathbf{R}^n \times (0,\infty),\ n = 2,3, \qquad u(x,0) = 0, \quad u_t(x,0) = \delta(x - x_0). \tag{1}$$

Equation (1) describes, e.g. propagation of acoustic and electromagnetic waves.

Let $\Omega \subset \mathbb{R}^n, n = 2,3$ be a convex bounded domain with the boundary $\partial\Omega \in C^n, n = 2,3$. We shall assume that $c(x)$ satisfies the following conditions:

$$\begin{cases} c(x) \in C^2(\mathbf{R}^n), \quad 2d_1 \le c(x) \le 2d_2, \quad d_1 > 0,\ d_2 > 0, \\ c(x) = 2d_1, \quad \text{for } x \in \mathbf{R}^n \setminus \Omega, \quad \Omega \subset \mathbf{R}^n, \quad n = 2,3, \end{cases} \tag{2}$$

where, d_1 and d_2 are given bounds for the function $c(x)$,

In this work we consider the case of the *backscattered* data, or such data which are given only at a part of the boundary of the computational domain. Let us define our computational domain Ω with the backscattered boundary Γ:

$$\Omega \subset \{x = (x_1, x_2, x_3) : x_3 > 0\},$$
$$\Gamma = \partial\Omega \cap \{x_3 = 0\} \neq \varnothing.$$

In our computations we will consider the case when the wave field is initialized by the incident plane wave propagating along the positive direction of the x_3-axis in the half space $\{x_3 < 0\}$ and "falling" on the half space $\{x_3 > 0\}$. Numerical tests in section 8 are performed for the given function g_0 and g_1, where $u(x,t) = g_1(x,t)$ at Γ and $u(x,t) = g_0(x,t)$ at $\partial\Omega \setminus \Gamma$, with $u(x,t)$ satisfying the Cauchy problem

$$\begin{aligned} u_{tt} - \Delta u = 0, \quad & \text{in } \Omega \times (0,\infty), \\ u(x,0) = 0,\ u_t(x,0) = f(x), \ & \text{in } \Omega. \end{aligned} \tag{3}$$

Hence, in these tests we set

$$u(x,t) := g_2(x,t) = \begin{cases} g_1(x,t), (x,t) \in \Gamma \times (0,\infty), \\ g_0, (x,t) \in (\partial\Omega \setminus \Gamma) \times (0,\infty) \end{cases} \tag{4}$$

and consider the following Inverse problem:

Inverse Problem with backscattered data (IPB). *Suppose that the coefficient $c(x)$ satisfies conditions (2) and it is unknown in the domain Ω. Determine the function $c(x)$ for $x \in \Omega$, assuming that the function $g_2(x,t)$ in (4) is known for a single direction of the incident plane wave propagating along the positive direction of x_3-axis in the half space $\{x_3 < 0\}$ and falling on the half space $\{x_3 > 0\}$*

We note that our formulation of IPB is for the case of a plane wave. In the case of problem (1), with a Dirac delta function as initial data, the formulation of Inverse Problem IPB is similar. In this case we should replace the wording "for a single direction of the incident plane wave propagating along the positive direction

of x_3-axis in the half space $x_3 < 0$ and falling on the half space $\{x_3 > 0\}$", by the expression "for a single source position $x_0 \in \{x_3 < 0\}$".

Next, we use the Laplace transform

$$U(x,s) = \int_0^\infty u(x,t)e^{-st}dt, \qquad \text{for } s > \underline{s} > 0, \tag{5}$$

where $\underline{s}$ is the *pseudo-frequency* constant. Recall that it suffices to choose $\underline{s}$ such that the integral (5) and its first partial derivatives in x and t converge. Then U satisfies

$$\begin{cases} \Delta U - s^2 c(x) U = -\delta(x - x_0)\, c(x_0), & \forall s \geq \underline{s} > 0, \\ \lim_{|x|\to\infty} U(x,s) = 0, & \forall s \geq \underline{s} > 0. \end{cases} \tag{6}$$

For every $s \geq \underline{s}$, the equation (6) possesses a positive, unique solution U.

2.1 The nonlinear integro-differential equation with eliminated unknown coefficient

Introducing the function $v = \ln U$, since $x_0 \notin \overline{\Omega}$, then (6) yields

$$\Delta v + |\nabla v|^2 = s^2 c(x), \qquad \text{in } \Omega, \tag{7}$$

$$v(x,s) = \ln G(x,s), \ \forall (x,s) \in \partial\Omega \times [\underline{s}, \overline{s}], \tag{8}$$

where $G(x,s)$ is the Laplace transform of the data function $g(x,t)$. To single out the unknown coefficient $c(x)$ in (7), we introduce a new function

$$H(x,s) = \frac{v}{s^2}. \tag{9}$$

Assuming certain regularity conditions ([6]), it follows that H satisfies

$$\Delta H + s^2 |\nabla H|^2 = c(x). \tag{10}$$

Next let

$$q(x,s) = \partial_s H(x,s), \tag{11}$$

then using (11)

$$H(x,s) = -\int_s^\infty q(x,\tau)\, d\tau := -\int_s^{\overline{s}} q(x,\tau)\, d\tau + W(x,\overline{s}), \tag{12}$$

where $\overline{s} > s_0$ is a large number and

$$W(x,\overline{s}) \approx H(x,\overline{s}) = \frac{\ln U(x,\overline{s})}{\overline{s}^2}. \tag{13}$$

$W(x,\overline{s})$ is known as the *tail function*. To determine W we need to choose the parameter $\overline{s}$ numerically. We include W either on the right hand side in iteration steps as data, or study it as an unknown in a coupled system of equations.

Differentiating (10) with respect to s, from (12)-(13), we obtain the following nonlinear integro-differential equation for $q = q(x,s)$,

$$\begin{aligned} \Delta q - 2s^2 \nabla q \cdot \int_s^{\overline{s}} \nabla q(x,\tau)\, d\tau + 2s \left[\int_s^{\overline{s}} \nabla q(x,\tau)\, d\tau \right]^2 \\ + 2s^2 \nabla q \nabla W - 2s \nabla W \cdot \int_s^{\overline{s}} \nabla q(x,\tau)\, d\tau + 2s (\nabla W)^2 = 0. \end{aligned} \tag{14}$$

By (8), (9) and (11) we may impose the following Dirichlet boundary condition

$$q(x,s) = \psi(x,s),\ \forall (x,s) \in \partial\Omega \times [\underline{s},\overline{s}]. \tag{15}$$

where ψ satisfies

$$\psi\Big(x,s\Big) = \frac{G_s}{Gs^2} - \frac{2\ln G}{s^3}. \tag{16}$$

Suppose that $D_x^\alpha q,\ |\alpha| \leq 2$ are already approximated. Then the coefficient $c(x)$ can be, approximately, determined using (10), where H is given by (12), which requires an initial guess for W as well.

3 A Sequence of elliptic Dirichlet boundary value problems

We approximate $q(x,s)$ with a piecewise constant function with respect to s. Assume a partition $\underline{s} = s_N < s_{N-1} < ... < s_1 < s_0 = \overline{s},\ s_{n-1} - s_n = k$ of $[\underline{s},\overline{s}]$ with a sufficiently small and uniform step size k such that $q(x,s) = q_n(x)$ for $s \in (s_n, s_{n-1})$. Hence,

$$\int_s^{\overline{s}} \nabla q(x,\tau) d\tau = (s_{n-1} - s)\nabla q_n(x) + k \sum_{j=1}^{n-1} \nabla q_j(x), \quad s \in (s_n, s_{n-1}). \tag{17}$$

We approximate the boundary condition (15) as being piecewise constant on s,

$$q_n(x) = \overline{q}_n(x), \quad x \in \partial\Omega, \quad j = 1,\ldots,n, \tag{18}$$

where

$$\overline{f}_n(x) = \frac{1}{k} \int_{s_n}^{s_{n-1}} f(x,s)\, ds. \tag{19}$$

On each subinterval $(s_n, s_{n-1}], n \geq 1$, we assume that $q_j(x),\ j = 1,...,n-1$ are known. In this way, for each n, $n = 1,\ldots,N$, we obtain an approximate equation for $q_n(x)$. Now we insert (17) in (14) and multiply the resulting equation by the Carleman Weight Function (CWF).

$$C_{n,\lambda}(s) = e^{\lambda(s-s_{n-1})}, \qquad s \in (s_n, s_{n-1}], \qquad \lambda >> 1, \tag{20}$$

and integrate over $s \in (s_n, s_{n-1}]$. (see Theorem 6.1 [6]). We obtain for $n = 1,...,N$,

$$\begin{aligned} \mathscr{L}_n\left(q_n, W_n\right) - \varepsilon q_n =: \Delta q_n - A_{1,n}\left(k\sum_{i=1}^{n-1}\nabla q_i\right)\nabla q_n + A_{1n}\nabla q_n \nabla W_n - \varepsilon q_n \\ \approx 2\tfrac{I_{1,n}}{I_0}\left(\nabla q_n\right)^2 - A_{2,n}k^2\Big(\sum_{i=1}^{n-1}\nabla q_i(x)\Big)^2 + 2A_{2,n}\nabla W_n\Big(k\sum_{i=1}^{n-1}\nabla q_i\Big) - A_{2,n}\Big(\nabla W_n\Big)^2. \end{aligned} \tag{21}$$

The term $-\varepsilon q_n$ is added for regularizing purpose. The coefficients are computed as:

$$\begin{aligned} I_0 : \quad &= \int_{s_n}^{s_{n-1}} C_{n,\lambda}(s)\,ds, \qquad I_{1,n} := \int_{s_n}^{s_{n-1}} s(s_{n-1}-s)[s-(s_{n-1}-s)] \\ A_{1,n} : &= \frac{2}{I_0}\int_{s_n}^{s_{n-1}} s[s-2(s_{n-1}-s)]C_{n,\lambda}(s)\,ds, \qquad A_{2,n} := \frac{2}{I_0}\int_{s_n}^{s_{n-1}} sC_{n,\lambda}(s)\,ds. \end{aligned}$$

Thus we have the Dirichlet boundary value problem (21), with the boundary data (18). In this system the tail function W is also unknown. Observe that,

$$\frac{|I_{1,n}(\lambda,k)|}{I_0(\lambda,k)} \leq \frac{4\bar{s}^2}{\lambda}, \qquad \text{for } \min(\lambda k, \bar{s}) \geq 1. \tag{22}$$

Therefore taking $\lambda >> 1$ we mitigate the influence of the nonlinear term with $(\nabla q_n)^2$ in (21), which enables us to solve a linear problem on each iterative step.

4 A finite element discretization

We approximate the solution for (21) by a finite element method with continuous piecewise linear functions on *a partially structured mesh* in space, and implement resulting scheme using a hybrid code. More specifically, we decompose the computational domain G into $\Omega \subset G$ and $\Omega^c = G \setminus \Omega$, and discretize Ω by an unstructured mesh and Ω^c by a quasi-uniform mesh. In Ω, for each n, we use a partition $\mathscr{T}_{n,h} = \{K\}$. Here $h = h(x)$ denotes a piecewise constant mesh function $h = h(x)$ representing the diameter of the element K containing x, and $(\cdot,\cdot)$ and $\|\cdot\|$, denote the L_2-inner product and norm, respectively.

Choosing $c(x) = 1$ for $x \in \Omega^c$, given $g(x,t) = u\,|_{\partial\Omega}$, we can uniquely determine the function $u(x,t)$ as the solution of the boundary value problem for equation (1) with boundary conditions on both boundaries ∂G and $\partial\Omega$. Next, using Laplace transform of $u(x,t)$, (9) and (11) one can uniquely determine $\tilde{q}(x)$,

$$\tilde{q}(x) =: \frac{\partial q}{\partial \mathbf{n}}\Big|_{\partial\Omega}, \tag{23}$$

here $\mathbf{n}$ is the outward unit normal to the boundary $\partial\Omega$ at the point $x \in \partial\Omega$. In our computations the functions $p(x,t), \tilde{q}(x)$ and $g(x,t)$ are calculated from the solution of the forward problem (21) with the exact value of the coefficient $c(x)$. A variational formulation for (21) is: for $n = 1,\dots,N$; find $V_n,\ q_n \in H^1(\Omega)$ such that

$$\begin{aligned}
&\mathscr{F}(q_n, V_n; \varphi) =: (\nabla q_n, \nabla\varphi) + (A_{1,n}(k\sum_{i=1}^{n-1}\nabla q_i)\nabla q_n, \varphi) - (A_{1n}\nabla q_n \nabla W_n, \varphi) + (\varepsilon q_n, \varphi)\\
&+(2\tfrac{I_{1,n}}{I_0}(\nabla q_n)^2, \varphi) - (A_{2,n}k^2(\sum_{i=1}^{n-1}\nabla q_i(x))^2, \varphi) + (2A_{2,n}\nabla W_n(k\sum_{i=1}^{n-1}\nabla q_i), \varphi)\\
&-(A_{2,n}(\nabla W_n)^2, \varphi) \approx (\tilde{q}_n, \varphi)_{\partial\Omega}, \quad \forall\varphi \in H^1(\Omega).
\end{aligned} \tag{24}$$

To formulate a finite element method for (21), we introduce the trial space $V^q_{n,h}$,

$$V^q_{n,h} := \{v_n \in H^1(\Omega) : v_n|_K \in P_1(K),\ \partial_{\mathbf{n}} v_n|_{\partial\Omega} = \tilde{q}_{n,h},\ \forall K \in \mathscr{T}_{n,h}\},$$

where $n = 1,\dots,N$, $P_1(K)$ denotes the set of linear functions on K and $\tilde{q}_{n,h}$ is an approximation for $\tilde{q}(x)$. We also introduce the test function space $V_{n,h}$ defined as

$$V_{n,h} := \{v_n : v_n \text{ is continuous on } \Omega, \text{ and } w_n|_K \in P_1(K), \quad \forall K \in \mathscr{T}_{n,h}\}.$$

$V_{n,h}$ and $V^q_{n,h} \subset H^1(\Omega)$. The finite element for (21) is formulated as: for $n = 1,\dots,N$, find $q_{n,h}$ and $W_{n,h} \in V^q_{n,h}$, approximations of q_n and W_n, respectively; such that

$$\mathscr{F}(q_{n,h}, W_{n,h}; \varphi) \approx (\tilde{q}_{n,h}, \varphi)_{\partial\Omega}, \quad \forall\varphi \in V_{n,h}. \tag{25}$$

subtracting (25) from (24) we get the classical *Galerkin orthogonality:*

$$\mathscr{F}(q_n, W_n; \varphi) - \mathscr{F}(q_{n,h}, W_{n,h}; \varphi) \approx 0, \quad \forall\varphi \in V_{n,h}. \tag{26}$$

Now, we introduce the residual, $\mathscr{R}_n := \mathscr{R}_n(q_{nh}, W_{n,h})$, for a discrete solution for (21) as follows: for $n = 1,\dots,N$; find $q_{nh}, W_{n,h} \in V^q_{n,h}$ such that

$$\begin{aligned}
&-\Delta_h q_{nh} + A_{1,n}\left(k\sum_{i=1}^{n-1}\nabla q_{ih}\right)\nabla q_{nh} - A_{1n}\nabla q_{nh}\nabla W_{nh} + \varepsilon q_{nh} + 2\tfrac{I_{1,n}}{I_0}(q_{nh})^2\\
&-A_{2,n}k^2\left(\sum_{i=1}^{n-1}\nabla q_{ih}(x)\right)^2 + 2A_{2,n}\nabla W_{nh}\left(k\sum_{i=1}^{n-1}\nabla q_{ih}\right) - A_{2,n}(\nabla W_{nh})^2 := \mathscr{R}_n,\\
&\quad q_{nh}|_{\partial\Omega} = \tilde{q},
\end{aligned} \tag{27}$$

where $\Delta_h q_{nh}$ denotes the discrete Laplacian defined by

$$(\Delta_h q_{nh}, \eta) = (\nabla q_{nh}, \nabla\eta), \qquad \forall\eta \in W_{n,h}. \tag{28}$$

Let now $e_{n,h} = q_n - q_{n,h},\ n = 1,\dots,N$, then a modified form of the Galerkin orthogonality (26), yields the strong error representation formula:

$$\begin{aligned} -\Delta_h e_{n,h} &+ I_1\nabla e_{n,h} + \varepsilon e_{n,h} + 2\tfrac{I_{1,n}}{I_0}\left[(\nabla q_n)^2 - (\nabla q_{n,h})^2\right] \\ &+ I_2\cdot(k\sum_{i=1}^{n-1}\nabla e_{i,h}) + I_3\cdot\nabla\Theta_n = -\mathscr{R}_n. \end{aligned} \tag{29}$$

For each interval $[s_n, s_{n-1})$, we rewrite (29) (we suppress n) and consider the equation

$$\begin{aligned} \Gamma e := -\Delta e + C_1\nabla e + \varepsilon e + \delta\Lambda e = -C_2\left(k\textstyle\sum_{i=1}^{n-1}\nabla e_i\right) - \mathscr{R} - C_3\nabla\Theta \\ e|_{\partial\Omega} = 0, \end{aligned} \tag{30}$$

where C_j, $j = 1,2,3$ are corresponding to the spatially continuous versions of I_j:s, $\delta := I_{1,n}/I_0$ and Λ, the nonlinear term, is defined by

$$\Lambda e := |\nabla q|^2 - |\nabla q_h|^2. \tag{31}$$

In (30) the error in W is included in the Θ-term and the residual term $\mathscr{R}$ satisfies

$$(\mathscr{R}, \varphi) \approx 0, \qquad \forall\varphi \in V_{n,h}. \tag{32}$$

5 Bounds for the nonlinear operator Λ and a priori estimates

Below we derive a bound for Λ, using $f(q) = |\nabla q|^2$, $0 < \theta < 1$, and

$$\begin{aligned} \mathscr{D}\ f(\theta q + (1-\theta)q_h) &= \mathscr{D}\Big(|\nabla(\theta q + (1-\theta)q_h)|^2\Big) \\ &= 2\Big(|\nabla(\theta q + (1-\theta)q_h)|\Big)\cdot\Big(\mathscr{D}|\nabla(\theta q + (1-\theta)q_h)|\Big), \end{aligned} \tag{33}$$

where $\mathscr{D}f$ is given in the Taylor expansion of $f(q_h)$ about q, viz:

$$f(q_h) = f(q) + (q_h - q)\mathscr{D}f(\theta q + (1-\theta)q_h). \tag{34}$$

We may write Λe in a compact form as

$$\Lambda e = 2e\Big(|\theta\nabla e + \nabla q_h|\Big)\cdot\Big(\mathscr{D}|\nabla(\theta q + (1-\theta)q_h)|\Big). \tag{35}$$

5.1 The dual problem for a linearized approach

Here, we sketch a framework for the dual approach for a *linear/linearized version* of (30). To begin with, we assume that Λ is a linear operator and let

$$\Gamma^\star\varphi := -\Delta\varphi - C_1\nabla\varphi + \varepsilon\varphi + \delta\Lambda^\star\varphi = e, \qquad n = 1,\dots,N, \qquad \varphi|_{\partial\Omega} = 0, \quad (36)$$

with $\Gamma^\star$ and $\Lambda^\star$ being the adjoints of Γ and Λ, respectively. By (30) we have that

$$\|e\|^2_{L_2(\Omega)} = (e, \Gamma^\star\varphi) = (\Gamma e, \varphi) = -(\tilde{\mathscr{R}}, \varphi). \quad (37)$$

The identity (37) is known as *the error representation formula*. Using the identities

$$-(\chi, \varphi - P_h\varphi) = -(\chi - P_h\chi, \varphi - P_h\varphi), \quad (38)$$

for $\chi = \mathscr{R}$, $\chi = C_2\sum_{i=1}^{n-1}\nabla e_i$, or $\chi = C_3\nabla\Theta$, where $P_h : L_2(\Omega) \to W_{n,h}$ is the $L_2(\Omega)$-projection, and we have used the orthogonality $\mathscr{R} \perp W_{n,h}$, and the strong stability estimates for the dual problem, we get from (37) (see [2] for details) that

$$\|e\|_{L_2(\Omega)} \le C_s C_i \left\|h^2(\tilde{\mathscr{R}} - P_h\tilde{\mathscr{R}})\right\| \le CC_s C_i \left\|h^2(\mathscr{R} - P_h\mathscr{R})\right\|, \quad (39)$$

where C_i and C_s are interpolation and stability constants respectively. Recalling (35)

$$(\Lambda^\star\varphi, e) = (\varphi, \Lambda e) = 2\Big(\varphi,\ \Big[|\theta\nabla e + \nabla q_n|\Big] \cdot \Big[\mathscr{D}|\nabla(\theta q + (1-\theta)q_h)|\Big] e\Big). \quad (40)$$

For piecewise linear approximation, successive use of Hölder inequality yields

$$|(\Lambda^\star\varphi, e)| \le C\|\varphi\|\,\|e\|\,\|q\|_{W^2_\infty}\Big(\|q_h\|_{W^1_\infty} + \|e\|_{W^1_\infty}\Big). \quad (41)$$

Thus we get the following estimate for the nonlinear operator Λ:

$$\|\Lambda\| \le \|q\|_{W^2_\infty}\Big(\|q_h\|_{W^1_\infty} + \|e\|_{W^1_\infty}\Big).$$

Theorem 1 (An a priori error bound). *Let $q_n \in W_2^2(\Omega)$ and q_{nh}, be the solutions for (24) and (25), respectively. Then for a piecewise linear finite element approximation error $e_n = q_n - q_{n,h}$ we have (see [2]) that*

$$\|e_n\| \le Ch\|q_n\|_{W_2^2} = \mathscr{O}(h). \quad (42)$$

6 A posteriori error estimation

The a posteriori error analysis is based on representing the error in terms of the solution φ of the dual problem, related to (21). We recall the problem (30) and write the dual problem for all $[s_n, s_{n-1})$, $n = 1,\dots,N$, as

$$-\Delta\varphi - C_1\nabla\varphi + \varepsilon\varphi + \delta\Lambda^\star\varphi + \delta\,|\nabla\varphi_h|^2 + \tilde{C}_{\varphi,\Theta} = \psi, \qquad \varphi|_{\partial\Omega} = 0, \quad (43)$$

where $\tilde{C}_{\varphi,\Theta} := C_2 k\sum_{i=1}^{n-1}\nabla\varphi_i + C_3\nabla\Theta$ is assumed to be known from the previous iteration steps, and $\Theta = \Theta_n = W_h - W_{n,h}$. We assume that $\Theta \in H^1_{loc}$ and $\varphi_h \in W^{1,4}_{loc}$. Thus,

we wish to control the quantity (e,ψ) with $e = q - q_h$ in Ω, where $\psi \in [L^2(\Omega)]^3$ is given. For approximations of spectral order > 1, (for linear approximation the J_5-term below will vanish) we may write

$$\begin{aligned}(\psi,e) \approx &-(\Delta\varphi,e) - (C_1\nabla\varphi,e) + (\varepsilon\varphi,e) - \delta(|\nabla q_h|^2\mathscr{D}(\varphi),e)\\ &+\delta(\mathscr{D}(|\nabla q_h|^2\varphi),e) + \delta(|\nabla\varphi_h|^2,e) + (\tilde{C}_{\varphi,\Theta},e) =: \textstyle\sum_{k=1}^{7} J_k.\end{aligned} \tag{44}$$

Due to the limited regularity of the approximate solution $q_{n,h}$, the scalar products $I_j,\ j = 1,\dots,7$, involving $e = q_n - q_{n,h}$, should be performed elementwise: $(f,g) := \sum_K (f,g)_K$. This will introduce accumulative sum of the normal derivatives over enter-element boundaries. Taking into account these boundary terms, by repeated use of Green's formula, we can recompute each $J_j,\ j = 1,\dots,7$, separately. In this way, finally we obtain the following error representation inequality:

Lemma 1. *Let φ be the solution of the dual problem (43), q that of (24), and q_h the FEM solution of (25). Then the following error representation inequality holds true:*

$$\big|(\psi,e)\big| \le (|\tilde{\mathscr{R}}_1|,|\sigma|) + (|\tilde{\mathscr{R}}_2|,|\sigma|) + C_3(|\nabla\Theta|,|e|) + \delta(|\nabla\varphi_h|^2,|e|), \tag{45}$$

where the residuals are defined as

$$\tilde{\mathscr{R}}_1 =: \Delta_h e - C_1\nabla e - \varepsilon e - \delta\Lambda e - C_2 k\sum_{i=1}^{n-1}\nabla e_i, \quad \tilde{\mathscr{R}}_2 = \max_{S\subset\partial K} h_K^{-1}\big|\big[\partial_s q_h\big]\big|, \tag{46}$$

and interpolation error is

$$\sigma = h_K\big[\partial_{\mathbf{n}}\varphi_h\big]. \tag{47}$$

Now we use, elementwise, Hölder inequality and Let $\psi = e$ to obtain the following a posteriori error estimate:

Theorem 2. *Let φ be the solution of the dual problem (43), q the solution of (24), and q_h the FEM solution of (25). Then there is a constant C, independent of Ω and h, such that for $\psi - \delta|\nabla\varphi_h|^2 = e$ the following a posteriori error estimate holds:*

$$\|e\|^2 \le Ch\Big[\Big(\|\mathscr{R}_1\|_{L_2(\Omega)} + \|\mathscr{R}_2\|_{L_2(\Omega)}\Big)\|\tilde{\sigma}\|_{L_2(\Omega)} + h|C_3|^2\Big], \tag{48}$$

where $h = \max_K(h_K)$, $\mathscr{R}_1 = \tilde{\mathscr{R}}_1(q_h) = \Delta_h q_h + C_1\nabla q_h - \varepsilon q_h - \delta\Lambda q_h - C_2 k\sum_{i=1}^{n-1}\nabla q_{h,i}$, $\mathscr{R}_2 = \tilde{\mathscr{R}}_2$ is given in (46), $\tilde{\sigma} = \big[\partial_{\mathbf{n}}\varphi_h\big]$, and $\mathscr{R}_3\Big|_K := |\nabla\Theta|\Big|_K$ can be estimated as $\|\mathscr{R}_3\|^2_{L_2(\Omega)} \approx C_\Omega\xi^2 \sim Ch^2$, whereas choosing $\psi := e + \delta|\nabla\varphi_h|^2 + C_3|\nabla\Theta|$ yields

$$\|e\|^2 \le Ch\Big(\|\mathscr{R}_1\|_{L_2(\Omega)} + \|\mathscr{R}_2\|_{L_2(\Omega)}\Big)\|\tilde{\sigma}\|_{L_2(\Omega)}. \tag{49}$$

7 The Adaptive Approximate Globally Convergent Algorithm

In this section we present our adaptive globally convergent algorithm, where we use Theorem 2 which states that the error, between the exact and approximate solution for the functions q_n of the equation (21), depends on the residuals given by (46). However, in the case of using continuous piecewise linear finite element approximation of functions q_n, only the first residual $\tilde{\mathscr{R}}_1$ will appear. To calculate it we should find an approximate solution q_n of the equation (21) on every mesh. We get q_n as $q_n = \lim_{k\to\infty} q_n^k$, where k is the number of iterations with respect to the tail function $W_n(x,\overline{s})$.

To solve equation (21) on a new refined mesh we first linearly interpolate the function $\overline{\psi}_n$, given by (15), for each pseudo-frequency interval $[s_n, s_{n-1})$. Then, on every mesh we compute approximations c_n of $c(x)$ using variational formulation of the equation (7), see [5] for full details. Thus, we can explicitly compute the function c_n on every frequency interval (s_n, s_{n-1}) through the finite element formulation.

We denote the stopping number k (on which these iterations are stopped) by m_n.

7.1 An Approximate Globally Convergent Algorithm

Below, we briefly describe a globally convergent algorithm of [5, 6, 8] which we use in our computations and in the adaptive globally convergent algorithm.

Step 0. $n_1, n \geq 1$. Stage 1: iterate with respect to the nonlinear term. Assume that the functions $q_1, ..., q_{n-1}, q_{n,1}^0 (:= q_{n-1}) \in C^{2+\alpha}(\overline{\Omega})$ and the tail function $V_{n,0}(x,\overline{s}) \in C^{2+\alpha}(\overline{\Omega})$ are already constructed. Then, we solve,iteratively, the following Dirichlet boundary value problems: For $k = 1, 2, ...$, find $q_{n,1}$ such that

$$\begin{aligned} \Delta q_{n,1}^k - A_{1n}\left(h\sum_{j=1}^{n-1}\nabla q_j\right)\cdot\nabla q_{n,1}^k - \varepsilon q_{n,1}^k + A_{1n}\nabla q_{n,1}^k\cdot\nabla W_{n,0} \\ = 2\tfrac{I_{1n}}{I_0}\left(\nabla q_{n,1}^{k-1}\right)^2 - A_{2n}h^2\left(\sum_{j=1}^{n-1}\nabla q_j(x)\right)^2 \\ +2A_{2n}\nabla W_{n,0}\cdot\left(h\sum_{j=1}^{n-1}\nabla q_j(x)\right) - A_{2n}(\nabla W_{n,0})^2, \\ q_{n,1}^k = \overline{\psi}_n(x), \qquad x\in\partial\Omega. \end{aligned} \tag{50}$$

As a result, we obtain the function $q_{n,1} := \lim_{k\to\infty} q_{n,1}^k$ in the $C^{2+\alpha}(\overline{\Omega})$.

Step 1. Compute $c_{n,1}$ via backwards calculations using finite element formulation of equation (7), see Chapter 3 of [5] for details.

Step 2. Solve the hyperbolic forward problem with $c_n(x) := c_{n,1}(x)$, calculate the Laplace transform and the function $U_{n,1}(x,\overline{s})$.

Step 3. Find a new approximation for the tail function

$$W_{n,1}(x)=\frac{\ln U_{n,1}(x,\overline{s})}{\overline{s}^2}. \tag{51}$$

Step 4. n_i, $i\geq 2$. We now iterate with respect to the tails (51). Suppose that functions $q_{n,i-1},W_{n,i-1}(x,\overline{s})\in C^{2+\alpha}\left(\overline{\Omega}\right)$ are already constructed.

Step 5. Solve the boundary value problem

$$\begin{aligned}\Delta q_{n,i}-A_{1n}\left(h\sum_{j=1}^{n-1}\nabla q_j\right)\cdot\nabla q_{n,i}-\kappa q_{n,i}+A_{1n}\nabla q_{n,i}\cdot\nabla W_{n,i-1}\\ =2\tfrac{I_{1n}}{I_0}\left(\nabla q_{n,i-1}\right)^2-A_{2n}h^2\left(\sum_{j=1}^{n-1}\nabla q_j(x)\right)^2\\ +2A_{2n}\nabla W_{n,i-1}\cdot\left(h\sum_{j=1}^{n-1}\nabla q_j(x)\right)-A_{2n}\left(\nabla W_{n,i-1}\right)^2,\\ q_{n,i}(x)=\overline{\psi}_n(x),\qquad x\in\partial\Omega.\end{aligned} \tag{52}$$

Step 6. Compute $c_{n,i}$ by backwards calculations using finite element formulation of equation (7), see Chapter 3 of [5].

Step 7. Solve the hyperbolic forward problem (1) with $c_n(x):=c_{n,i}$, compute the Laplace transform and obtain the function $W_{n,1}(x,\overline{s})$.

Step 8. Find a new approximation for the tail function

$$W_{n,i}(x)=\frac{\ln U_{n,i}(x,\overline{s})}{\overline{s}^2}. \tag{53}$$

Step 9. Iterate with respect to i and stop iterations at $i=m_n$ such that $q_{n,m_n}:=\lim_{i\to\infty}q_{n,i}^k$. Stopping criterion for computing functions $q_{n,i}^k$ is

$$\text{either } F_n^k\geq F_n^{k-1} \text{ or } F_n^k\leq\eta, \tag{54}$$

where η is a chosen tolerance and F_n^k are defined as

$$F_n^k=\frac{||q_{n,i}^k-q_{n,i}^{k-1}||_{L_2(\Gamma)}}{||q_{n,i}^{k-1}||_{L_2(\Gamma)}}$$

Step 10. Set

$$q_n:=q_{n,m_n},\qquad c_n(x):=c_{n,m_n}(x),\qquad W_{n+1,0}(x):=\frac{\ln W_{n,m_n}(x,\overline{s})}{\overline{s}^2}.$$

Step 11. We stop computing functions $c_{n,i}^k$ when

$$\text{either}\quad N_n\geq N_{n-1} \text{ or}\quad N_n\leq\eta, \tag{55}$$

where

$$N_n = \frac{||c^k_{n,i} - c^{k-1}_{n,i}||_{L_2(\Omega)}}{||c^{k-1}_{n,i}||_{L_2(\Omega)}}. \tag{56}$$

7.2 Adaptive Approximate Globally Convergent Algorithm

In computations of section 8 we use the following adaptive approximate globally convergent algorithm:

Step 0. Choose an initial mesh K_h in Ω and an initial time partition J_0 of the time interval $(0,T)$. Compute an initial approximation c^0_{n,m_n} using an approximate globally convergent algorithm described above on the initial mesh, see [5] for the details. Compute the sequence of functions c^j_{n,m_m}, where $j > 0$ is the number of mesh refinements, on adaptively refined meshes via following steps:

Step 1. Compute the initial approximation for the tail function $W_n(x,\overline{s})$ on a new mesh K_h using the computed solution of the hyperbolic problem (3).

Step 2. Compute the finite element solutions $q^j_n(x,s)$ of equation (21) on a refined mesh K_h on the pseudo-frequency interval (s_n, s_{n-1}) using Algorithm of section 7.1.

Step 3. Update the coefficient c^j_n on K_h using the finite element formulation for (7).

Step 4. Stop computing c^j_n and obtain the function c^j_{n,m_n} using the criterion (55).

Step 5. Refine the mesh at all the points where

$$c^j_{n,m_n}(x) \geq \beta_1 \max_{\Omega} c^j_{n,m_n}. \tag{57}$$

The tolerance number $\beta_1 \in (0,1)$ is chosen by the user.

Step 6. Construct a new refined mesh K_h in Ω and a new time partition J_τ of the time interval $(0,T)$ satisfying the CFL condition, and return to step 1 and perform all of the above steps on the new mesh.

Step 7. Stop mesh refinements and obtain the function c^j_{n,m_n} if norms defined in the criterion (55) are fullfilled.

8 Imaging of land mines using an adaptive approximate globally convergent algorithm

In this section we present numerical implementation of an adaptive approximate globally convergent method with backscattered data in two dimensions. Our goal is reconstruction of land mines from backscattered data using an adaptive approximate globally convergent algorithm of section 7.2.

Let the ground be $\{\mathbf{x}=(x,z): z>0\}\subset\mathbb{R}^2$. Suppose that a polarized electric field is generated by a plane wave, which is initialized at the line $\{z=z^0<0, x\in\mathbb{R}\}$ at the moment of time $t=0$.

In our model we use the well-known fact that the maximal depth of an antipersonnel land mine does not exceed approximately 10 centimeters (cm)=0.1 meter (m), and we model these mines as small rectangles with length of side 0.2 meter and width of side 0.1 meter. In our computations we are interested in imaging of land mines when one mine is located very close to the other one. This is an important case in the real-life military applications.

We have modelled such a problem on a domain Ω, see Figure 1, viz: We set

$$\widetilde{\Omega}_{FEM}=\{\mathbf{x}=(x,z)\in(-0.3,0.3)\ \mathrm{m}\times(0.05,0.45)\mathrm{m}\},$$

and introduce a dimensionless spatial variables $\mathbf{x}'=\mathbf{x}/(0.1m)$, so that the domain $\widetilde{\Omega}_{FEM}$ is transfered into a dimensionless computational domain

$$\Omega_{FEM}=(-3.0,3.0)\times(0.5,4.5).$$

We choose values of function $c(x)$ using tables of dielectric constants [35], and use the fact that in the dry sand $c=5$ and in the trinitrotoluene (TNT) $c=22$. Thus, the relation of mine/background contrast is $22/5\approx 4$, hence we consider new parameters

$$c'=\frac{c}{5},$$

to get

$$c(\text{dry sand})=1,\ c(\text{TNT})\approx 4. \tag{58}$$

For simulation of backscattered data for the inverse problem IPB, we solve the forward problem using the software package WavES [36]. The dimensionless size of our computational domain is $\Omega=[-4.0,4.0]\times[0,5.0]$. This domain is split into a dimensionless finite element domain $\Omega_{FEM}=[-3.0,3.0]\times[0.5,4.5]$ and a surrounding domain Ω_{FDM} with a structured mesh, $\Omega=\Omega_{FEM}\cup\Omega_{FDM}$, see Figure 1. The spatial mesh in Ω_{FEM} and in Ω_{FDM} the mesh consists of triangles and squares, respectively. The mesh size is $\widetilde{h}=0.125$ in the overlapping regions. The boundary of the domain Ω is $\partial\Omega=\partial\Omega_1\cup\partial\Omega_2\cup\partial\Omega_3$. Here, $\partial\Omega_1$ and $\partial\Omega_2$ are respectively top and bottom sides of the domain Ω, see Figure 1, and $\partial\Omega_3$ is the union of left and right sides of this domain. We define the boundary of the domain Ω_{FEM} as $\Gamma=\Gamma_1\cup\Gamma_2\cup\Gamma_3$. Here, Γ_1 and Γ_2 are respectively top and bottom sides of the domain Ω_{FEM}, see Figure 1, and Γ_3 is the union of left and right sides of this domain.

We use the hybrid method of [10]. Since in our applications we know value of the coefficient $c(\mathbf{x})$ outside of the domain of interest Ω_{FEM} such that

$$c(\mathbf{x})=1 \text{ in } \Omega_{FDM}, \tag{59}$$

hence we need to determine $c(\mathbf{x})$ only in Ω_{FEM}.

The forward problem in our computational test is

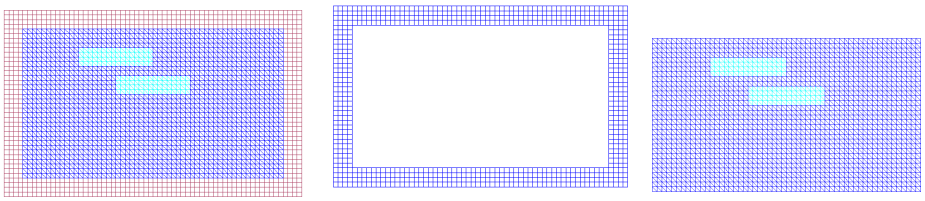

a) $\Omega = \Omega_{FEM} \cup \Omega_{FDM}$ b) Ω_{FDM} c) Ω_{FEM}

Fig. 1 *a) Geometry of the hybrid mesh. This is a combination of the quadrilateral mesh in the subdomain Ω_{FDM} b), where we apply FDM, and the finite element mesh in the inner domain Ω_{FEM} c), where we use FEM. The solution of the inverse problem is computed in Ω_{FEM}. The trace of the solution of the forward problem (60) is recorded at the top boundary Γ_1 of the finite element domain Ω_{FEM}.*

$$\begin{aligned} c(\mathbf{x})\, u_{tt} - \Delta u = 0, \quad & \text{in } \Omega \times (0,T), \\ u(\mathbf{x},0) = 0,\ u_t(\mathbf{x},0) = 0, \ & \text{in } \Omega, \\ \partial_n u = f(t), \ & \text{on } \partial\Omega_1 \times (0,t_1], \\ \partial_n u = -\partial_t u, \ & \text{on } \partial\Omega_1 \times (t_1,T), \\ \partial_n u = -\partial_t u, \ & \text{on } \partial\Omega_2 \times (0,T), \\ \partial_n u = 0, \ & \text{on } \partial\Omega_3 \times (0,T), \end{aligned} \tag{60}$$

where $f(t)$ is the amplitude of the initialized plane wave,

$$f(t) = \frac{(\sin(\omega t - \pi/2) + 1)}{10}, \quad 0 \le t \le t_1 := \frac{2\pi}{\omega}. \tag{61}$$

To compute the data for the inverse problem we solve the forward problem (60) with $\omega = 7.0$ in (61) and in the time $T = (0,6)$ with the time step $\tau = 0.01$ which is satisfied the CFL condition, and save the solution of this problem at the top boundary Γ_1 of the finite element domain Ω_{FEM}. Figures 2 shows isosurfaces of the computed solution of the problem (60) in the computational domain Ω.

In our test we also define the set of admissible coefficients for the function $c(\mathbf{x})$ in Ω_{FEM} as

$$M_c = \{c(\mathbf{x}) : c(\mathbf{x}) \in [1,8],\ c(\mathbf{x}) = 1\ \forall \mathbf{x} \in \mathbb{R}^2 \setminus \Omega, c(\mathbf{x}) \in C^2\left(\mathbb{R}^2\right).\}$$

8.1 Numerical Results

We have performed two set of tests. In the first test we solve IPB using approximate globally convergent algorithm of section 7.1, and in the second test we solve IPB using adaptive approximate globally convergent algorithm of section 7.2. The goal of both tests was to reconstruct structure given on Figure 1-a).

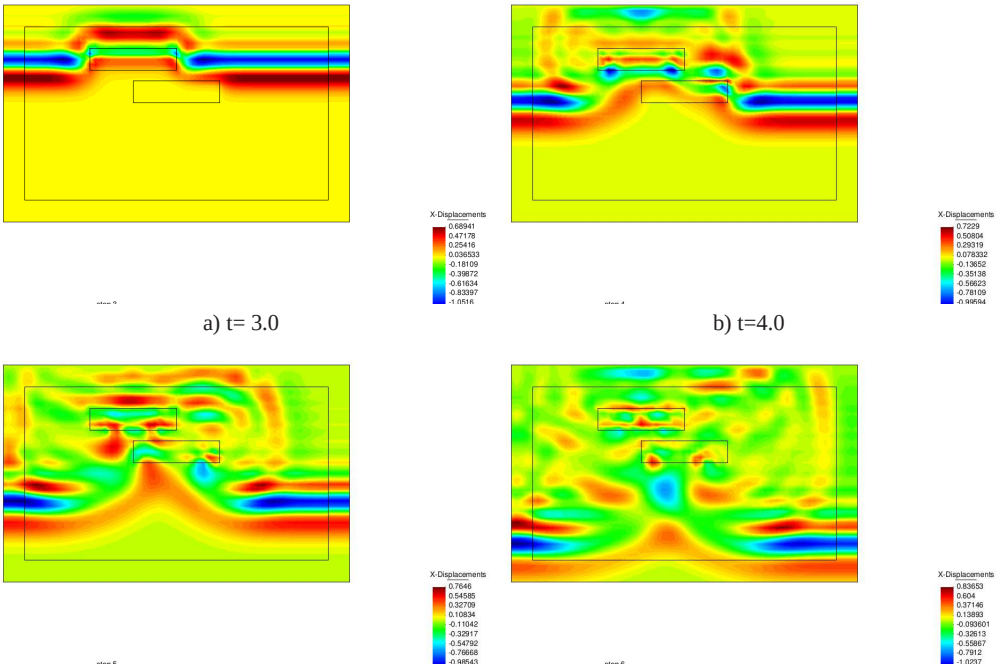

a) t= 3.0 b) t=4.0

c) t=5.0 d) t=6.0

Fig. 2 *Isosurfaces of the computed exact solution for the forward problem (60) at different times with a plane wave initialized at the top boundary.*

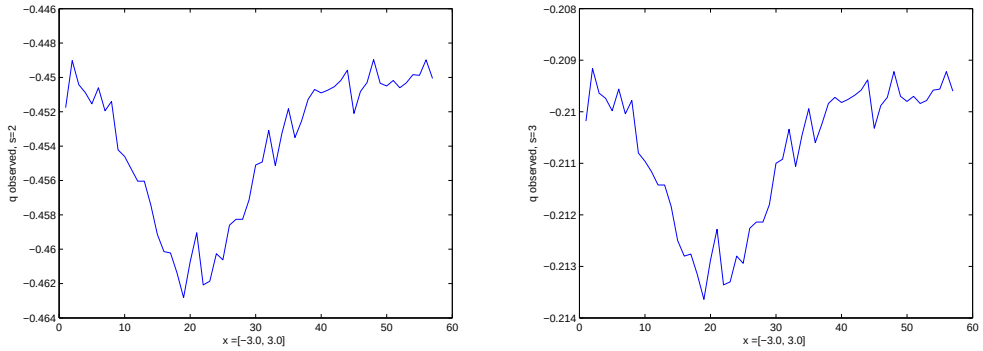

a) $s = 2$ b) $s = 3$

Fig. 3 *Backscattered data for the function q at the top boundary Γ_1 of the computational domain Ω_{FEM} computed for the different values of the pseudo-frequency s.*

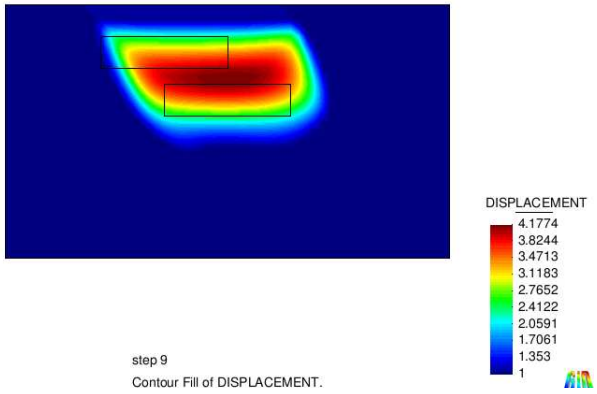

a) Test 1: $c_{7,9} \approx 4.17$

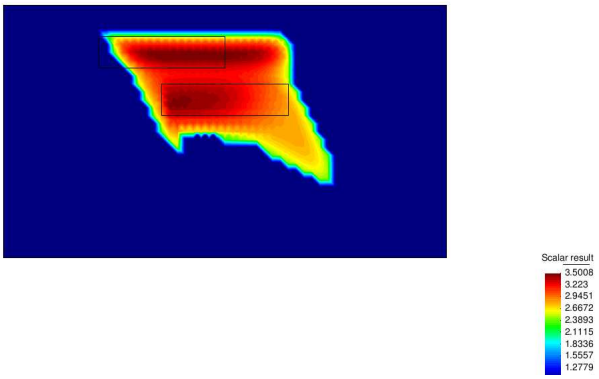

b) Test 2: $c^1_{5,4} \approx 3.5$

Fig. 4 *Computed images using backscattered data obtained from the geometry presented on Figure 1-a). a) Test1: location and contrast of inclusions are accurately imaged. b) Test2: location, contrast and shape of inclusions are accurately imaged. The computed function $c = 1$ outside of imaged inclusions.*

The backscattered data at the boundary Γ_1 in both tests were computationally simulated using the software package WavES [36] via solving the hyperbolic problem (60) with known values of the coefficient $c = 4$ inside two inclusions of Figure 1-a) and with 5% additive noise in simulated data.

Figure 3 displays sensitivity of the simulated function $q(\mathbf{x},s), \mathbf{x} \in \Gamma_1$ for $s = 2$ and $s = 3$. We observed, that all values of the function $|q(\mathbf{x})|$ for $s > 5$ are very noisy and does not show sensitivity to the inclusions. Because of that we decided to take pseudo-frequency interval $s = [2,3]$, where the computed function $q(\mathbf{x},s), \mathbf{x} \in \Gamma_1$ is most sensitive to the presence of two inclusions. We run both tests with the step in the pseudo-frequency $h = 0.05$.

8.2 Test 1

In this test we solve IPB using globally convergent algorithm of section 7.1. The boundary conditions for the integral-differential equation (50) were replaced with the following Dirichlet boundary conditions

$$q_n|_{\Gamma_1} = \psi_{1n}(\mathbf{x}),\ q_n|_{\Gamma_2 \cup \Gamma_3} = \psi_{2n}(\mathbf{x}),$$

where function $\psi_{1n}(\mathbf{x})$ and $\psi_{2n}(\mathbf{x})$ are generated by functions $g_1(\mathbf{x},t)$ and $g_0(\mathbf{x},t)$, respectively, defined in (4). In this test we simulated the function $g_0(\mathbf{x},t)$ at $\Gamma_2 \cup \Gamma_3$ by solution of the forward problem (60) with $c(\mathbf{x}) = 1$ at every point of the computational domain Ω. The Dirichlet boundary condition at $\Gamma_2 \cup \Gamma_3$ is also approximated and it is necessary to solve the integral-differential equation (50).

An approximate globally convergent algorithm of section 7.1 was used to calculate the image of Figure 4-a). We observe that the location of both mine-like targets is reconstructed accurately and the contrast $\max[c_{comp}(\mathbf{x})] = 4.17$ is also accurately imaged (exact $c(x) = 4$ in both inclusions).

However, in this test we were not able to separate images for both mines. We could only image them as one big inclusion. In the next test we try to improve the result of the reconstruction of the Test 1 using an adaptivity technique inside approximately globally convergent method.

8.3 Test 2

In this test we solve IPB using an adaptive globally convergent algorithm of section 7.2. This algorithm was used to calculate the image of Figure 4-b) which was obtained on the one time refined mesh. We observe that not only location and contrast of both mine-like targets are reconstructed accurately, but also the shape of mines is imaged more accurately than in the Test 1: in the Test 2 we are able to separate these two mines. Thus, we conclude that an adaptive approximate globally convergent algorithm of section 7.2 allows better reconstruction of shape of inclusions than an usual approximate globally convergent method of Section 7.1 even for the case of backscattered data.

Acknowledgments

The research of the authors was supported by the Swedish Research Council, the Swedish Foundation for Strategic Research (SSF) in Gothenburg Mathematical Modelling Centre (GMMC) and by the Swedish Institute, Visby Program.

References

1. H. Ammari, E. Iakovleva, and D. Lesselier, Music-type electromagnetic imaging of a collection of small threedimensional inclusions. *SIAM J.Sci.Comp.*, 29:674 709, 2007.
2. M. Asadzadeh and L. Beilina, A posteriori error analysis in a globally convergent numerical method for a hyperbolic coefficient inverse. *Inverse Problem* 26 (2010).
3. A.B. Bakushinsky and M.Yu. Kokurin, *Iterative Methods for Approximate Solution of Inverse Problems*, Springer, 2005.
4. L. Beilina, K. Samuelsson and K. Åhlander, Efficiency of a hybrid method for the wave equation. In *International Conference on Finite Element Methods*, Gakuto International Series Mathematical Sciences and Applications. Gakkotosho CO., LTD, 2001.
5. L. Beilina and M.V. Klibanov, *Approximate global convergence and adaptivity for Coefficient Inverse Problems*, Springer, New-York, 2012.
6. L. Beilina and M. V. Klibanov, A globally convergent numerical method for a coefficient inverse problem, *SIAM J. Sci. Comp.*, 31(1):478-509, 2008.
7. L. Beilina and M. V. Klibanov. A posteriori error estimates for the adaptivity technique for the Tikhonov functional and global convergence for a coefficient inverse problem. *Inverse Problems*, 26, 2010.
8. L. Beilina and M. V. Klibanov. Synthesis of global convergence and adaptivity for a hyperbolic coefficient inverse problem in 3D, *J. Inverse and Ill-posed problems*, 18(1), 2010.
9. L. Beilina and M.V. Klibanov, Reconstruction of dielectrics from experimental data via a hybrid globally convergent/adaptive inverse algorithm, *Inverse Problems*, 26, 125009, 2010.
10. L. Beilina, K. Samuelsson, and K. Åhlander, Efficiency of a hybrid method for the wave equation. In *Inter- national Conference on Finite Element Methods*, Gakuto International Series Mathematical Sciences and Applications. Gakkotosho CO.,LTD, 2001.
11. M. I. Belishev, Boundary control in reconstruction of manifolds and metrics (the bc method). *Inverse Problems*, 13, R1-R45, 1997.
12. M. I. Belishev and V. Yu Gotlib, Dynamical variant of the bc-method: theory and numerical testing. *Inverse and Ill-Posed Problems*, 7:221 240, 1999.
13. Budak B M, Samarskii A A and Tikhonov A N 1988 *A Collection of Problems in Mathematical Physics* (New York: Dover Publications)
14. V. A. Burov, S. A. Morozov, and O. D. Rumyantseva, Reconstruction of ne-scale structure of acoustical scatterers on large-scale contrast background. *Acoustical Imaging*, 26:231 238, 2002.
15. M. Cheney and D. Isaacson, Inverse problems for a perturbed dissipative half-space. *Inverse Problems*, 11:865 888, 1995.
16. H. W. Engl, M. Hanke, and A. Neubauer, *Regularization of Inverse Problems*. Kluwer Academic Publishers, Boston, 2000.
17. B. Engquist and A. Majda, Absorbing boundary conditions for the numerical simulation of waves. *Math. Comp.*, 31:629 651, 1977.
18. K. Eriksson and D. Estep and C. Johnson, *Computational Differential Equations*, Studentlitteratur, Lund, 1996.
19. C. Johnson, A. Szepessy, Adaptive finite element methods for conservation laws based on a posteriori error estimation, *Comm.Pure Appl.Math.*, 199–234, 1995.

20. M. V. Klibanov and A. Timonov, *Carleman Estimates for Coefficient Inverse Problems and Numerical Appli- cations.* VSP, Utrecht, The Netherlands, 2004.
21. M. V. Klibanov, Inverse problems and Carleman estimates, *Inverse Problems*, V. 8, 575–596, 1991.
22. M.V. Klibanov, M.A. Fiddy, L. Beilina, N. Pantong and J. Schenk, Picosecond scale experimental verification of a globally convergent numerical method for a coefficient onverse problem, *Inverse problems*, 26(3), 2010.
23. M. Klibanov and A. A. Timonov, A unified framework for constructing of globally convergent numerical algorithms for multidimensional coefficient inverse problems, *Applicable Analysis*, 83:933-955, 2004.
24. A. V. Kuzhuget and M. V. Klibanov, Global convergence for a 1-D inverse problem with application to imaging of land mines, *Applicable Analysis*, 89:1, 125-157, 2010.
25. O. A. Ladyzhenskaya and N. N. Uralceva, *Linear and Quasilinear Elliptic Equations*, Academic Press, New York, 1969
26. O. A. Ladyzhenskaya, *Boundary Value Problems of Mathematical Physics*, Springer Verlag, Berlin, 1985
27. J. L. Lions and E. Magenes, **Problèmes aux limites non homogènes et applications.** Vol. 1. (French) Travaux et Recherches Mathématiques, No. 17 Dunod, Paris 1968 xx+372 pp.
28. J. Mueller and S. Siltanen, Direct reconstructions of conductivities from boundary measurements. *SIAM J. Sci. Comp.*, 24:1232 1266, 2003.
29. A. Nachman, Global uniqueness for a two-dimensional inverse boundary value problem. *Annals of Mathematics*, 143:71 96, 1996.
30. J. Nitsche, *Direct proofs of some unusual shift-theorems*, Analyse mathématique et applications, 383–400, Gauthier-Villars, Montrouge, 1988.
31. R. G. Novikov, Multidimensional inverse spectral problem for the equation .. + (v(x) .. eu(x)) = 0. *Functional Analysis and Its Applications*, 22:11 22, 1988.
32. R. G. Novikov, The $\overline{\partial}$ approach to approximate inverse scattering at xed energy in three dimensions. *Inter- national Math. Research Papers*, 6:287 349, 2005.
33. V. G. Romanov, *Inverse Problems of Mathematical Physics*, VNU, Utrecht, The Netherlands, 1986
34. A. N. Tikhonov and V. Y. Arsenin, *Solutions of Ill-Posed Problems.* Winston and Sons, Washington, DC, 1977.
35. Tables of dielectric constants at http://www.asiinstr.com/technical/DielectricConstants.htm.
36. Software package WavES at http://www.waves24.com/